Hypochlorite and superoxide radicals can act synergistically to induce fragmentation of hyaluronan and chondroitin sulphates

Martin D. REES, Clare L. HAWKINS and Michael J. DAVIES[1]

Free Radical Group, Heart Research Institute, Camperdown, Sydney, NSW 2050, Australia

Activated phagocytes release the haem enzyme MPO (myeloperoxidase) and also generate superoxide radicals ($O_2^{\bullet-}$), and hence H_2O_2, via an oxidative burst. Reaction of MPO with H_2O_2 in the presence of chloride ions generates HOCl (the physiological mixture of hypochlorous acid and its anion present at pH 7.4). Exposure of glycosaminoglycans to a MPO–H_2O_2–Cl^- system or reagent HOCl generates long-lived chloramides [R-NCl-C(O)-R′] derived from the glycosamine *N*-acetyl functions. Decomposition of these species by transition metal ions gives polymer-derived amidyl (nitrogen-centred) radicals [R-N$^\bullet$-C(O)-R′], polymer-derived carbon-centred radicals and site-specific strand scission. In the present study, we have shown that exposure of glycosaminoglycan chloramides to $O_2^{\bullet-}$ also promotes chloramide decomposition and glycosaminoglycan fragmentation. These processes are inhibited by superoxide dismutase, metal ion chelators and the metal ion-binding protein BSA, consistent with chloramide decomposition and polymer fragmentation occurring via $O_2^{\bullet-}$-dependent one-electron reduction, possibly catalysed by trace metal ions. Polymer fragmentation induced by $O_2^{\bullet-}$ [generated by the superoxide thermal source 1, di-(4-carboxybenzyl)hyponitrite] was demonstrated to be entirely chloramide dependent as no fragmentation occurred with the native polymers or when the chloramides were quenched by prior treatment with methionine. EPR spin-trapping experiments using 5,5-dimethyl-1-pyrroline-*N*-oxide and 2-methyl-2-nitrosopropane have provided evidence for both $O_2^{\bullet-}$ and polymer-derived carbon-centred radicals as intermediates. The results obtained are consistent with a mechanism involving one-electron reduction of the chloramides to yield polymer-derived amidyl radicals, which subsequently undergo intramolecular hydrogen atom abstraction reactions to give carbon-centred radicals. The latter undergo fragmentation reactions in a site-specific manner. This synergistic damage to glycosaminoglycans induced by HOCl and $O_2^{\bullet-}$ may be of significance at sites of inflammation where both oxidants are generated concurrently.

Key words: chloramide, glycosaminoglycan, hypochlorite, myeloperoxidase, radical, superoxide.

INTRODUCTION

Activated phagocyte cells have been shown to release the haem enzyme MPO (myeloperoxidase) and are also known to generate superoxide radicals ($O_2^{\bullet-}$) and its dismutation product H_2O_2 via an oxidative burst. Reaction of MPO with H_2O_2 in the presence of chloride ions generates a mixture of HOCl and its anion (pK_a 7.59; HOCl is used hereafter to designate the physiological mixture of these species). HOCl is a potent bactericide and plays an important role in mammalian defences against invading microorganisms. However, there is now considerable evidence that excessive or misplaced generation of HOCl may play a role in the development of a number of human inflammatory diseases including atherosclerosis, rheumatoid arthritis, periodontal disease and proteinuric glomerulopathies [1–4].

The reaction of HOCl with proteins, DNA and glycosaminoglycans has been shown to produce polymer-derived chloramine (R-NCl-H) and chloramide [R-NCl-C(O)-R′] species as a result of the reaction of HOCl with amine and amide functions [5–10]. For the glycosaminoglycans hyaluronan and chondroitin sulphate, chloramides are the major species formed due to the high concentration of N-acetyl groups (on glucosamine or galactosamine residues) in the repeating disaccharide units of these polymers [11]. Decomposition of glycosaminoglycan chloramides to polymer-derived amidyl [R-N$^\bullet$-C(O)-R′] radicals has been shown to initiate site-specific polysaccharide fragmentation [10]. Low-valent transition metal ions (e.g. Cu^+ or Fe^{2+}) stimulate this process by one-electron reduction of the chloramides [10]. Evidence has been obtained from both EPR studies and product analyses for the rearrangement of these polymer-derived amidyl radicals via intramolecular hydrogen atom abstraction to yield polymer-derived carbon-centred radicals and that further reaction of these radicals via O_2-dependent and -independent processes results in strand scission (Scheme 1) [10]. Protein chloramines have also been shown to react with low-valent transition metal ions and with $O_2^{\bullet-}$; these reactions lead to the formation of nitrogen-centred radicals and backbone fragmentation [12].

Glycosaminoglycans, such as hyaluronan and chondroitin sulphates, are important components of ECM (extracellular matrix) and modulate a variety of cellular and tissue functions [13]. These negatively charged polysaccharides avidly bind the positively charged (cationic) MPO [14–17] and hence are likely to be important targets for MPO-derived oxidants. Glycosaminoglycans also form stable complexes with transition metal ions, such as Cu^{2+} [18,19], which can catalyse glycosaminoglycan chloramide decomposition [10,20]. Evidence has been obtained that HOCl induces fragmentation of glycosaminoglycans in cultured ECM, and in ECM isolated from pig aortae, via the formation and subsequent decomposition of polymer-derived chloramides to radicals [20].

In the present study, we have examined the hypothesis that $O_2^{\bullet-}$ might enhance the decomposition of glycosaminoglycan chloramides via one-electron reduction (either directly or via a metal-ion-mediated process) to form polymer-derived amidyl radicals and, consequently, initiate strand scission. The induction of damage to glycosaminoglycans in this manner may be of

Abbreviations used: DMPO, 5,5-dimethyl-1-pyrroline-*N*-oxide; DTBN, di-*tert*-butylnitroxide; ECM, extracellular matrix; MNP, 2-methyl-2-nitrosopropane; MPO, myeloperoxidase; SOD, superoxide dismutase; SOTS-1, superoxide thermal source 1, di-(4-carboxybenzyl)hyponitrite; TNB, 5-thio-2-nitrobenzoic acid; XO, xanthine oxidase.

[1] To whom correspondence should be addressed (e-mail m.davies@hri.org.au).

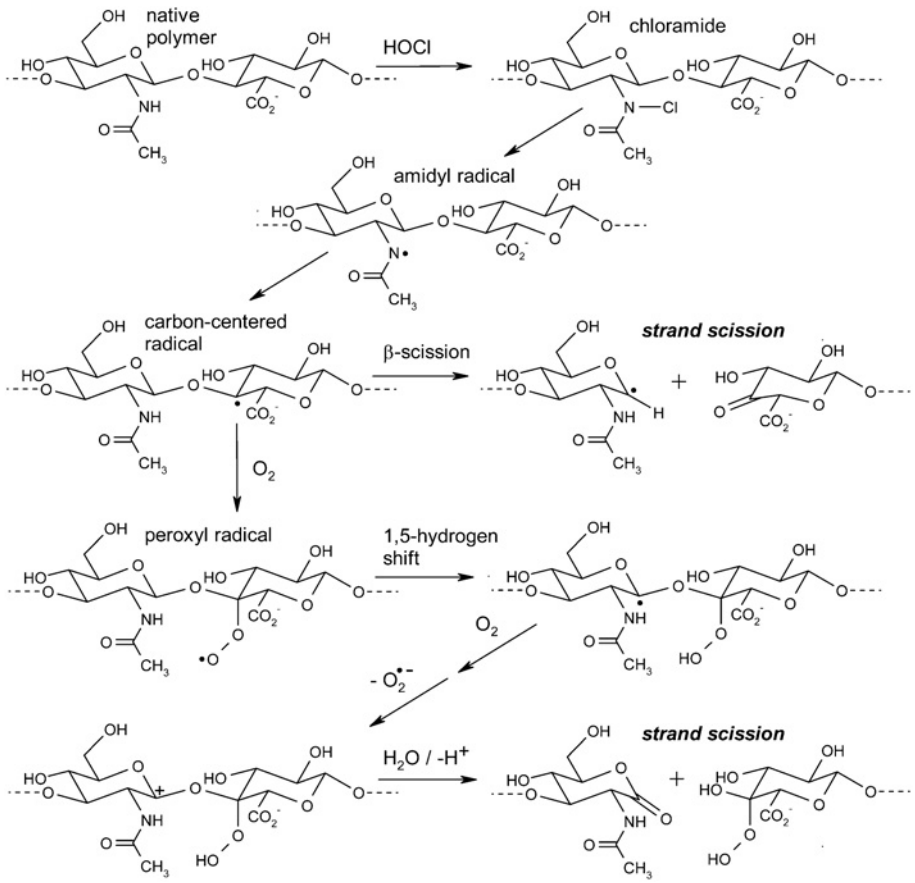

Scheme 1 HOCl-induced glycosaminoglycan fragmentation (hyaluronan-derived species are shown)

Extensions of the partial structures shown are indicated by dashed bonds. Evidence for the mechanisms depicted has been presented in [10].

considerable biological importance since $O_2^{\bullet-}$ and MPO-derived HOCl are generated concurrently by activated phagocytes [21].

EXPERIMENTAL

Materials

Solutions were prepared using water filtered through a four-stage Milli Q system. pH control was achieved using 0.1 M phosphate buffer (pH 7.4) treated with washed Chelex resin (Bio-Rad Laboratories, Hercules, CA, U.S.A.) to remove contaminating trace metal ions. Sodium hyaluronate (hyaluronan; 120 kDa) was obtained from Genzyme (Cambridge, MA, U.S.A.). Chondroitin sulphate A (chondroitin-4-sulphate, from whale cartilage, 25–50 kDa) was obtained from Seikagaku (Chuo-Ku, Tokyo, Japan). Copper-zinc SOD (superoxide dismutase, from bovine erythrocytes, S-2515), XO (xanthine oxidase, X-4500), BSA (A-6003), potassium superoxide (KO_2) and DMSO (spectrophotometric grade) were obtained from Sigma (St. Louis, MO, U.S.A.) and used as supplied. The SOTS-1 (superoxide thermal source 1), di-(4-carboxybenzyl)hyponitrite [22], was a gift from Professor C. Easton (Research School of Chemistry, Australian National University, Canberra, Australia). DMPO (5,5-dimethyl-1-pyrroline-*N*-oxide; ICN, Seven Hills, NSW, Australia) was purified before use by treatment with activated charcoal. Stock solutions of MNP (2-methyl-2-nitrosopropane) were made up in acetonitrile (CH_3CN) and diluted into the final reaction mixture such that the final concentration of CH_3CN was $\leqslant 10\%$ (v/v). HOCl solutions were prepared by dilution of a concentrated stock (0.5 M in 0.1 M NaOH) in 0.1 M (pH 7.4) phosphate buffer, with the HOCl concentration determined spectrophotometrically at pH 12 using the molar absorption coefficient ε_{292} of 350 $M^{-1} \cdot cm^{-1}$ [23]. All other chemicals were of analytical grade.

Three $O_2^{\bullet-}$ sources were employed in these studies: (i) SOTS-1 ($\leqslant$ 1.34 mM SOTS-1, 37 °C, pH 7.4), (ii) KO_2 in DMSO/50 mM crown-18 polyether [$\leqslant$ 4.54 mM final concentration of KO_2 (see below), 22 °C, pH 7.4] and (iii) an aerobic acetaldehyde (CH_3CHO)–XO system ($\leqslant$ 4.9 mM CH_3CHO, 0.93–0.97 unit/ml XO, 22 °C, pH 7.4). SOTS-1 undergoes slow decomposition at 37 °C and pH 7.0 ($t_{1/2} = 4900$ s) to yield $O_2^{\bullet-}$ in approx. 40% yield [22,24]. Stock solutions of KO_2 ($\leqslant$ 50 mM) in DMSO/50 mM crown-18 polyether (360 μl) were infused into stirred aqueous solutions (3600 μl) through poly(tetrafluoroethylene) syringe needles at a rate of 4 μl/min; the reported concentrations of KO_2 in the paper refer to the final concentrations of KO_2 that would be present if the stock solution were added as a bolus. Acetaldehyde was selected as a substrate for XO, as xanthine (one of the natural substrates for XO) is a purine, and such compounds react rapidly with HOCl [7] and probably react with chloramides, thereby giving rise to artifacts (cf. reaction of NADH with chloramides [25]).

Assay of chloramides

TNB (5-thio-2-nitrobenzoic acid; 35–45 μM, prepared as described previously [26,27]) was used to quantify the yield of

chloramides after 15 min reaction using ε_{412} 13600 $M^{-1} \cdot cm^{-1}$ [27]. No interference with the TNB assay was observed with SOTS-1 (freshly prepared or decomposed), DMSO/crown-18 polyether or any components of the CH_3CHO–XO system. KO_2-infused solutions slightly oxidized the TNB reagent in the absence of chloramides (with this attributed to the presence of H_2O_2), giving rise to a small, positive error in the determination of chloramide concentrations ($\leqslant 10\ \mu M$).

EPR

EPR spectra were recorded at room temperature (21 °C) using a Bruker EMX X-band spectrometer with 100 kHz modulation and a cylindrical ER4103TM cavity. Samples were contained in a flattened, aqueous sample cell (WG-813-SQ; Wilmad, Buena, NJ, U.S.A.) and spectral recording was initiated within 2–30 min of addition of the $O_2^{\bullet-}$ source and/or spin trap. Experiments were performed using glycosaminoglycan chloramides from which excess HOCl was removed by size-exclusion chromatography (PD10 columns; Amersham Biosciences, Uppsala, Sweden) to avoid direct reaction of HOCl with DMPO [28]. Hyperfine couplings were measured directly from the field scan and confirmed by computer simulation using the program WINSIM (available at http://EPR.niehs.nih.gov). Typical EPR spectrometer settings were: gain, 1×10^5; modulation amplitude, 0.02 mT; time constant, 0.16 s; scan time, 84 s; resolution, 1024 points; centre field, 384 mT; field scan, 10 mT; power, 25 mW; frequency, 9.76 GHz; 2–8 scans averaged.

PAGE

Samples were analysed using 20 % polyacrylamide gels and Alcian Blue staining as described previously with Bromophenol Blue as a tracking dye [10]. Aliquots (40 μl) from reaction mixtures were treated with 5 μl of 200 mM methionine at room temperature for 30 min to quench residual chloramides, and stored at − 18 °C before analysis. Gels were scanned and digitized over a linear range using a Bio-Rad Gel Doc 1000 system and associated software (Bio-Rad Laboratories).

The electrophoretic mobility of hyaluronan and chondroitin-4-sulphate chains is inversely proportional to the log of their molecular mass over a wide molecular mass range [29,30]. Therefore a loss of the parent band and a shift in staining towards the bottom of the gel represents a decrease in molecular mass. Digestion of hyaluronan and chondroitin-4-sulphate with testicular hyaluronidase produces a homologous series of oligosaccharides that differ only in their disaccharide content; these digests are visualized on polyacrylamide gels as 'ladders' and can be used as a molecular mass scale. The smallest oligosaccharides stained by Alcian Blue in polyacrylamide gels are the hyaluronan 8-disaccharide (with subsequent silver staining) [29] and the chondroitin-4-sulphate 3-disaccharide [30]. Exhaustive and partial digests of hyaluronan and chondroitin-4-sulphate (prepared as described in [31] and [30] respectively) were co-analysed in adjacent lanes in the above manner with Bromophenol Blue as tracking dye. The bands corresponding to the hyaluronan 8-disaccharide and the chondroitin-4-sulphate 3-disaccharide were identified as the fastest migrating bands in the exhaustive digests. Counting upwards from these bands, the bands corresponding to the hyaluronan 18-disaccharide and the chondroitin-4-sulphate 12-disaccharide were located. The relative fronts of these oligosaccharides compared with Bromophenol Blue (Rf_{BPB}) were then calculated: hyaluronan 18-disaccharide, $Rf_{BPB} = 0.51$; chondroitin-4-sulphate 12-disaccharide, $Rf_{BPB} = 0.83$. In subsequent gels, the migration distances of these oligosaccharides were calculated by multiplying the measured migration distance of Bromophenol Blue by the appropriate Rf_{BPB} value.

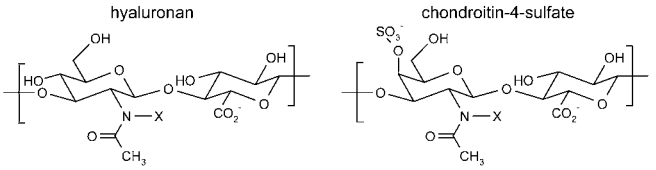

Figure 1 Structures of native glycosaminoglycans and glycosaminoglycan chloramides

X=H, native glycosaminoglycan; X=Cl, glycosaminoglycan chloramide.

Statistical analyses

Statistical analyses were performed using a GraphPad Prism software package (GraphPad Software, San Diego, CA, U.S.A.) with either one- or two-way ANOVA and post-hoc testing.

RESULTS

Preparation of glycosaminoglycan chloramides

Chloramide derivatives of hyaluronan and chondroitin-4-sulphate (see Figure 1 for structures) were prepared as described previously by reaction with HOCl at 37 °C [10]. Briefly, hyaluronan (3.65 mg/ml; approx. 9.1 mM amide groups) and chondroitin-4-sulphate (4.6 mg/ml; approx. 9.0 mM amide groups) were incubated with HOCl (45.5 mM) at 37 °C for 16 min; excess HOCl was subsequently removed by size-exclusion (PD10) chromatography. This methodology yielded chloramide concentrations, as assayed by TNB, of approx. 0.7 and 1.6 mM for chondroitin-4-sulphate and hyaluronan respectively, representing approx. 16 and 35 % conversion of the polymer N-acetyl amide functions into chloramides.

Decomposition of glycosaminoglycan chloramides in the absence and presence of $O_2^{\bullet-}$

The stability of the chloramide derivatives of hyaluronan and chondroitin-4-sulphate was examined at 37 °C and pH 7.4, under aerobic conditions in the absence or presence of added agents over 2–24 h using the TNB assay. Under these conditions, both glycosaminoglycan chloramides were stable in the absence of added agents (Figure 2), consistent with previous results [10]. Inclusion of SOTS-1 [di-(4-carboxybenzyl)hyponitrite, a thermal source of $O_2^{\bullet-}$] stimulated the decomposition of the glycosaminoglycan chloramides in a time- and concentration-dependent manner (Figure 2). The time course of this decomposition is in accordance with the expected rate of $O_2^{\bullet-}$ generation from SOTS-1 under these conditions ($t_{1/2}$ 4900 s at 37 °C and pH 7.0; [22]). The total chloramide losses induced after complete decomposition of SOTS-1 (370–1230 μM at 24 h) were close to or exceeded the theoretical yields of $O_2^{\bullet-}$ (550 μM). SOTS-1 that had been decomposed before its addition (by incubation at 37 °C for 24 h) did not induce chloramide decomposition (results not shown). With 1.34 mM SOTS-1, the inclusion of SOD (196 units/ml; 0.05 mg/ml) protected against SOTS-1-induced decomposition of hyaluronan chloramides (Figure 3A), whereas the inclusion of inactivated SOD (heated at > 95 °C for 10 min) did not (results not shown). Inclusion of EDTA (500 nM) or BSA (0.05 mg/ml)

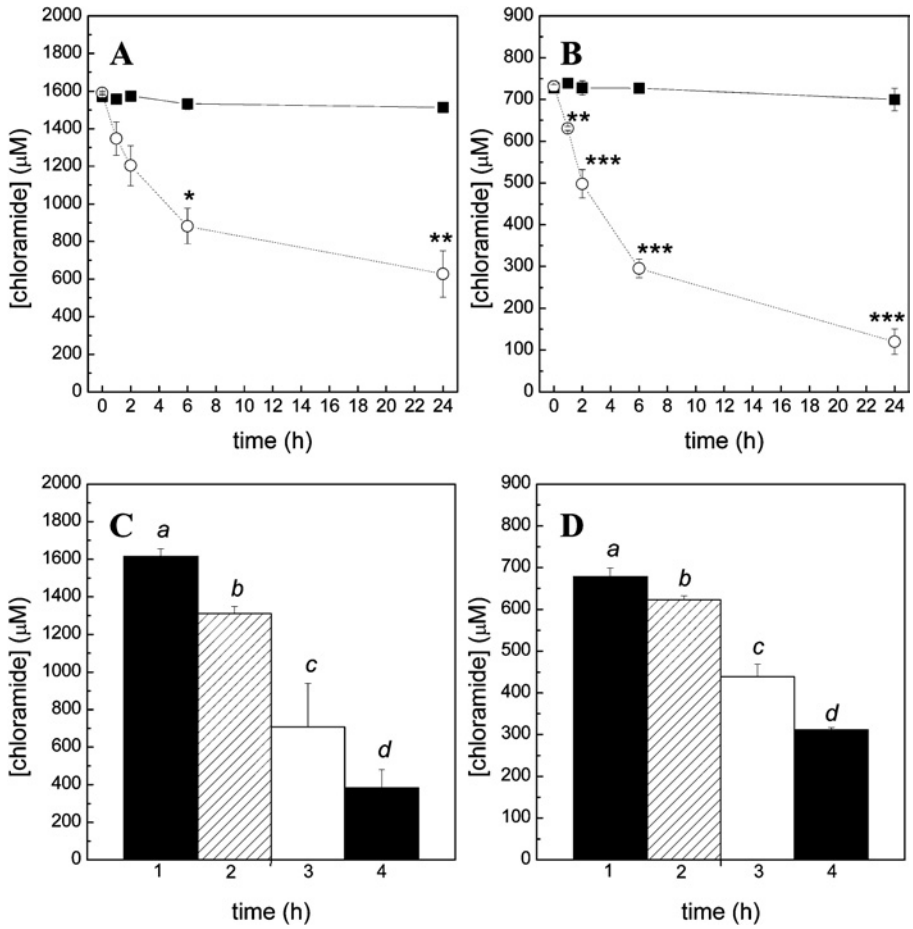

Figure 2 Time- and concentration-dependent decomposition of glycosaminoglycan chloramides induced by the $O_2^{\bullet-}$ source SOTS-1 at 37 °C and pH 7.4

(**A**) Hyaluronan chloramides with 0 (■) or 1.34 mM SOTS-1 (○). (**B**) Chondroitin-4-sulphate with 0 (■) or 1.34 mM SOTS-1 (○). (**C**) Hyaluronan chloramides with 0 (column 1), 0.134 (column 2), 0.67 (column 3) or 1.34 mM SOTS-1 (column 4) after 24 h incubation. (**D**) Chondroitin-4-sulphate chloramides with 0 (column 1), 0.134 (column 2), 0.67 (column 3) or 1.34 mM SOTS-1 (column 4) after 24 h incubation. All results are means ± S.D. ($n = 3$). In (**A**, **B**), $^*P < 0.05$, $^{**}P < 0.01$ and $^{***}P < 0.001$ indicate significant difference between the treatments (two-way ANOVA, Bonferroni post-hoc test). In (**C**, **D**), columns with different letters are significantly different from each other at the $P < 0.05$ level (one-way ANOVA, Newman–Keuls post-hoc test).

under identical reaction systems also resulted in significant decreases in the extent of hyaluronan chloramide decomposition induced by SOTS-1 (Figures 3B and 3C). SOD, EDTA and BSA exerted analogous protective effects against SOTS-1-induced decomposition of chondroitin-4-sulphate chloramides (results not shown). SOD, heat-inactivated SOD, EDTA and BSA alone had no effect on the stability of either of the glycosaminoglycan chloramides (results not shown).

KO_2 stimulated decomposition of hyaluronan chloramides (1210 μM) in a concentration-dependent manner at 22 °C and pH 7.4 (180, 340 and 470 μM chloramides decomposed in the presence of 0.91, 2.27 and 4.54 mM KO_2 respectively); neither DMSO nor crown-18 polyether affected the stability of the chloramides.

An aerobic CH_3CHO–XO system (4.9 mM CH_3CHO, 0.97 unit/ml XO, 22 °C, pH 7.4, 30 min) also stimulated decomposition of the glycosaminoglycan choramides [hyaluronan chloramides (1160 μM): 370 μM decomposed; chondroitin-4-sulphate chloramides (490 μM): 200 μM decomposed].

The effect of the nitrone spin-trap DMPO on the ability of $O_2^{\bullet-}$ sources to induce chloramide decomposition was examined, as DMPO is known to react, albeit slowly, with $O_2^{\bullet-}$ [32]. DMPO (102 mM) exerted partial protection against chloramide decomposition induced by SOTS-1 (1.09 mM SOTS-1, 37 °C, pH 7.4, 2 h incubation) and the CH_3CHO–XO system (4.0 mM CH_3CHO, 0.93 unit/ml XO, 22 °C, pH 7.4, 30 min incubation; approx. 50 % inhibition in each case). DMPO alone did not induce detectable chloramide decomposition after 30 min incubation at 22 °C; however, this agent induced a low extent of chloramide decomposition (240 μM) after 2 h incubation at 37 °C. Equivalent experiments were performed with the nitroso spin-trap MNP (20.4 mM, from a stock prepared in CH_3CN). MNP alone did not affect the stability of the chloramides. With the above-mentioned $O_2^{\bullet-}$ sources, similar extents of chloramide decomposition (approx. 100–300 μM) were observed in the presence of acetonitrile alone and in the presence of MNP.

Detection of radicals from glycosaminoglycan chloramides by EPR spin trapping in the absence or presence of $O_2^{\bullet-}$

Incubation of chondroitin-4-sulphate chloramides (680 μM) with CH_3CHO (4.0 mM) and XO (0.93 unit/ml) in the presence of DMPO (102 mM) at 22 °C and pH 7.4 resulted in the detection of broad, anisotropic EPR signals and a number of (minor) sharp, isotropic EPR signals (Figure 4A). The broad EPR signals are assigned to polymer-derived carbon-centred radical adducts with

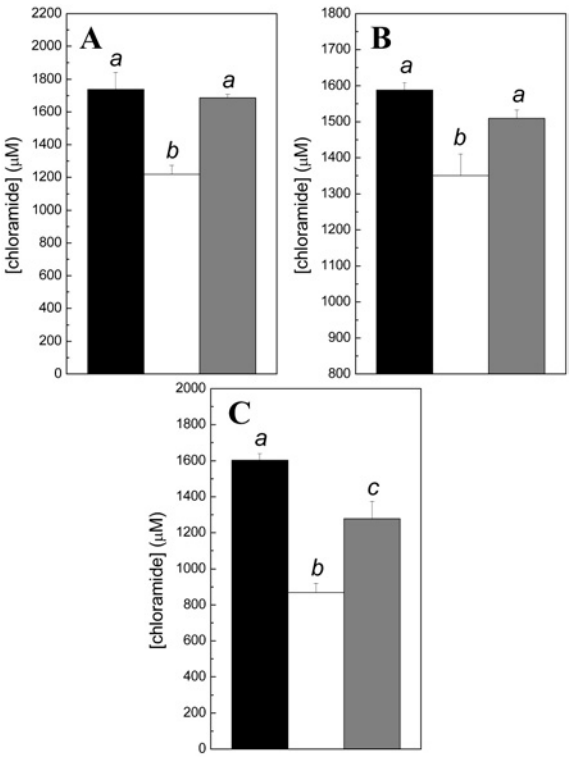

Figure 3 Inhibition of $O_2^{\bullet-}$-dependent decomposition of glycosaminoglycan chloramides by SOD, EDTA and BSA at 37 °C and pH 7.4

(**A**) Hyaluronan chloramides (black columns), hyaluronan chloramides with 1.34 mM SOTS-1 (white columns) or hyaluronan chloramides with 1.34 mM SOTS-1 and 196 units/ml SOD (0.05 mg/ml) (grey columns) after 2 h incubation. (**B**) As in (**A**), except that 500 nM EDTA is used instead of SOD. (**C**) As in (**A**), except 0.05 mg/ml BSA is used instead of SOD. All results are means ± S.D. ($n = 3$). Columns with different letters are significantly different from each other at the $P < 0.05$ level (one-way ANOVA, Newman–Keuls post-hoc test).

a(N) approx. 1.5–1.7 and $a(\beta$-H) approx. 2.2–2.4 mT (cf. results for similar adducts in [10]). Analysis of sequential EPR spectra obtained 2–30 min after initiation of the reaction showed that most of the polymer-derived radical adducts were generated in the first 2 min of the reaction. The isotropic EPR signals are assigned to DMPO-O_2H [a(N) 1.43, $a(\beta$-H) 1.17 and $a(\gamma$-H) 0.13 mT] and DMPO-OH [a(N) 1.49 and $a(\beta$-H) 1.49 mT] and adducts of acetaldehyde-derived radicals {DMPO-CH_3 [a(N) 1.62 and $a(\beta$-H) 2.32 mT] and DMPO-$COCH_3$ [a(N) 1.52 and $a(\beta$-H) 1.87 mT]} as observed previously with the CH_3CHO–XO system [33]. The same isotropic signals were observed after exposure of the native polymer to the complete reaction system in the presence of DMPO; however, no polymer-derived radical adducts were detected (Figure 4B). No polymer-derived radicals were detected after incubation of the chondroitin-4-sulphate chloramides in the absence of the enzyme and CH_3CHO (Figure 4C). Similar behaviour was observed in equivalent experiments with hyaluronan chloramides and hyaluronan (results not shown).

In equivalent experiments with MNP (20.4 mM) as spin trap, exposure of both glycosaminoglycan chloramides to the CH_3CHO–XO system resulted in the detection of broad, anisotropic EPR signals and two isotropic EPR signals (Figure 4D). The broad EPR signals are assigned to polymer-derived carbon-centred radical adducts with a(N) approx. 1.5–1.6 and a further, partially resolved doublet (hydrogen) hyperfine coupling a(H) approx. 0.3 mT; this splitting is particularly noticeable on the low-field (left-hand) and central sets of features. The signals with this additional coupling are assigned to adducts of radicals with the partial structure $^{\bullet}$CHRR′. Similar adducts of polymer-derived radicals, with the partial structure $^{\bullet}$CHRR′ [a(N) 1.55 and $a(\beta$-H) 0.31 mT], have been detected previously on metal ion-promoted decomposition of glycosaminoglycan chloramides in the presence of MNP [10]. The isotropic EPR signals are assigned to the one-electron reduction product of MNP, MNP-H [a(N) 1.45 and $a(\beta$-H) 1.39 mT] [34] and DTBN [di-*tert*-butylnitroxide: a(N) 1.71 mT] [34]. These isotropic signals were also observed with the native polymer; however, the polymer-derived radical adducts were not (Figure 4E). No polymer-derived radicals were detected after incubation of the hyaluronan chloramides in the absence of the enzyme and CH_3CHO (Figure 4F). Similar behaviour was observed in equivalent experiments with chondrotin-4-sulphate chloramides and chondroitin-4-sulphate (results not shown).

In contrast with the results obtained using DMPO with the CH_3CHO–XO system, neither $O_2^{\bullet-}$ or polymer-derived radicals were detected after incubation of 1.09 mM SOTS-1 (37 °C, pH 7.4, 30 min) with 102 mM DMPO in the presence or absence of the glycosaminoglycan chloramides or the native polymers. Instead, a signal [a(N) 1.45, $a(\beta$-H) 1.02 and $a(\gamma$-H) 0.14 mT] was detected in each case, which is assigned to the adduct of a SOTS-1-derived alkoxyl radical [$^{\bullet}$OC(H)OH-Ph-CO_2^-] formed after decomposition of the DMPO adduct of the SOTS-1-derived α-hydroxybenzylperoxyl radical [$^{\bullet}$OOC(H)OH-Ph-CO_2^-] (M. D. Rees, C. L. Hawkins and M. J. Davies, unpublished work). The failure to detect $O_2^{\bullet-}$ or polymer-derived radicals in the above experiments is probably due to trapping of SOTS-1-derived radicals [e.g. α-hydroxybenzylperoxyl radical, $^{\bullet}$OOC(H)OH-Ph-CO_2^-] by DMPO competing successfully with the generation of $O_2^{\bullet-}$ and/or the slow rate of $O_2^{\bullet-}$ formation from SOTS-1 under these conditions, relative to the stability of the resulting spin adducts.

Incubation of the glycosaminoglycan chloramides in the presence of SOTS-1 and MNP resulted in the detection of very weak, broad, anisotropic signals a(N), approx. 1.5–1.6 mT (results not shown) plus a number of isotropic EPR signals. The weak nature of these broad signals precluded further analysis. The isotropic EPR signals (but not the broad signals) were also observed after incubation of SOTS in the presence of MNP alone, and are assigned to the one-electron reduction product of MNP, MNP-H [a(N) 1.45 and $a(\beta$-H) 1.39 mT], DTBN [a(N) 1.71 mT] and SOTS-1-derived carbon-centred radical adducts [a(N) 1.53, $a(\beta$-H) 0.24 mT and a(N) 1.58, $a(\beta$-H) 0.16 mT]. The carbon-centred radical adducts are probably isomeric adducts of the $^{\bullet}$C(H)OH-Ph-CO_2^- radical formed during the decomposition of SOTS-1 (M. D. Rees, C. L. Hawkins and M. J. Davies, unpublished work).

Fragmentation of glycosaminoglycan chloramides in the absence or presence of $O_2^{\bullet-}$

The effect of $O_2^{\bullet-}$ on the structural integrity of the glycosaminoglycan chloramides, as assessed by PAGE, was investigated by incubation of these materials in the absence and presence of SOTS-1 at 37 °C and pH 7.4 under aerobic conditions over 2–24 h. Whereas little or no polymer fragmentation was detected on incubation of the glycosaminoglycan chloramides alone (as observed previously [10]), the inclusion of SOTS-1 (0.134–1.34 mM) induced polymer fragmentation in a time- and concentration-dependent manner (Figure 5). The rate and extent of this fragmentation is consistent with the rate and extent of chloramide decomposition detected in these incubations (cf. Figure 2). When fragmentation of chondroitin-4-sulphate was extensive, regular banding was observed on the lower portions

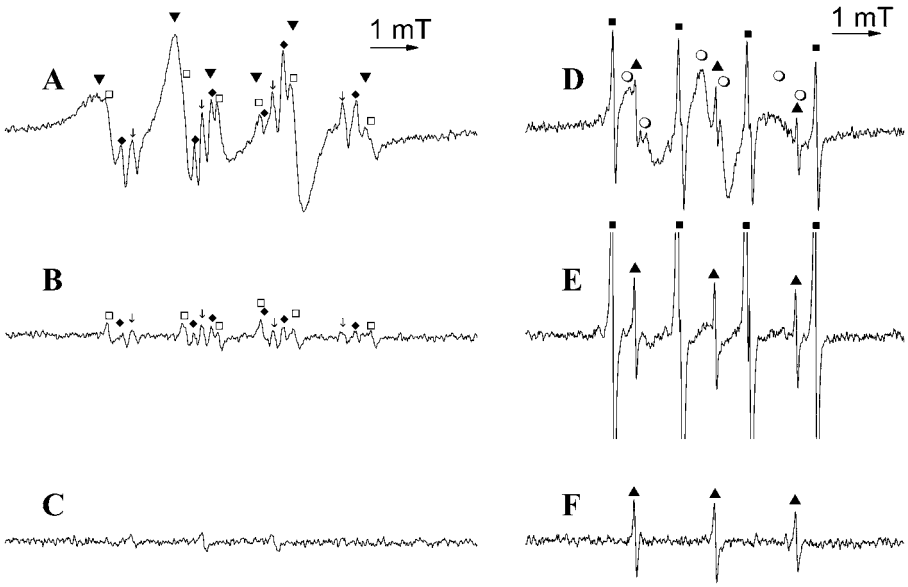

Figure 4 EPR spectra of spin adducts generated on exposure of chondroitin-4-sulphate chloramides and chondroitin-4-sulphate to $O_2^{\bullet-}$ in the presence of DMPO (A–C) and MNP (D–F)

Incubations contained 4.0 mM CH_3CHO, 0.93 unit/ml XO, 102 mM DMPO or 20.4 mM MNP at 22 °C and pH 7.4; spectra shown were acquired after 30 min incubation. Spectrum **A**, chondroitin-4-sulphate chloramides (680 μM) with complete system; spectrum **B**, chondroitin-4-sulphate with complete system; spectrum **C**, chondroitin-4-sulphate chloramides (680 μM) with no CH_3CHO or XO. Component signals in spectra **A**–**C** are denoted and assigned as follows: ▼, DMPO adducts of polymer-derived, carbon-centred radicals; (↓), DMPO-OH; ◆, DMPO-CH_3; and □, DMPO-$COCH_3$. Spectrum **D**, hyaluronan chloramides (680 μM) with complete system; spectrum **E**, hyaluronan with complete system; spectrum **F**, hyaluronan chloramides (680 μM) with no CH_3CHO or XO. Component signals in spectra **D**–**F** are denoted and assigned as follows: ○, MNP adducts of polymer-derived, carbon-centred radicals with the partial structure •CHRR′; ▲, MNP-H; ■, DTBN.

of gels (results not shown), consistent with the occurrence of site-specific fragmentation as detected in metal-ion-catalysed reactions [10]. With extensively fragmented hyaluronan samples, a low degree of staining was observed, as very low-molecular-mass hyaluronan oligosaccharides do not readily bind Alcian Blue [31]. No polymer fragmentation was detected in analogous incubations with the native glycosaminoglycans (results not shown) or with the glycosaminoglycan chloramides that had been quenched by prior reaction with excess methionine (Figures 6A and 6E). SOTS-1 that had been decomposed (by incubation at 37 °C for 24 h) before its addition did not induce fragmentation (results not shown). SOD (196 units/ml; 0.05 mg/ml), EDTA (500 nM) and BSA (0.05 mg/ml) protected against SOTS-1-induced fragmentation of the glycosaminoglycan chloramides (Figures 6B–6D and 6F–6H), but heat-inactivated SOD did not (results not shown). Methionine, SOD, inactivated SOD, EDTA and BSA alone had no effect on the structural integrity of the glycosaminoglycan chloramides (Figures 6A–6H, lane 2 in each case; results for inactivated SOD not shown).

KO_2 (0.91–4.54 mM) induced fragmentation of hyaluronan chloramides (1210 μM) in a concentration-dependent manner but did not induce detectable fragmentation of the native polymer (results not shown).

Exposure of both glycosaminoglycan chloramides (hyaluronan chloramides, 1160 μM and chondroitin-4-sulphate chloramides, 490 μM) to an aerobic CH_3CHO–XO system (4.9 mM CH_3CHO, 0.97 unit/ml XO, 22 °C, pH 7.4, 30 min) also gave rise to polymer fragmentation (Figures 7A and 7B, lane 3 in each case). In contrast with SOTS-1 and KO_2, this $O_2^{\bullet-}$ source also induced fragmentation of the native polymers (Figures 7A and 7B, lane 7 in each case); however, the extent of this fragmentation was less than that observed with the glycosaminoglycan chloramides.

The effects of the nitrone spin-trap DMPO and the nitroso spin-trap MNP on the ability of $O_2^{\bullet-}$ sources to induce fragmentation of the glycosaminoglycan chloramides were also examined. DMPO (102 mM) exerted partial protection against fragmentation of the glycosaminoglycan chloramides induced by the CH_3CHO–XO system (4.0 mM CH_3CHO, 0.93 unit/ml XO, 22 °C, pH 7.4, 30 min incubation) (Figures 7A and 7B) and SOTS-1 (1.09 mM SOTS-1, 37 °C, pH 7.4, 2 h incubation) (results not shown). No fragmentation was observed in the presence of DMPO alone. With the above-mentioned $O_2^{\bullet-}$ sources, similar extents of fragmentation were observed in the presence of acetonitrile alone and in the presence of MNP (results not shown).

DISCUSSION

In the present study, it has been shown that $O_2^{\bullet-}$ stimulates the decomposition of glycosaminoglycan chloramides, resulting in the formation of polymer-derived carbon-centred radicals and polymer fragmentation. The results obtained are consistent with the initial formation of (undetected) polymer-derived amidyl radicals after one-electron reduction of the chloramides, mediated either directly or indirectly, by $O_2^{\bullet-}$ (Scheme 2). The reactions of glycosaminoglycan-derived amidyl radicals have been examined in detail in a previous report [10]. Those studies have provided evidence for the formation of C-4 carbon-centred radicals on the uronic acid residues, and subsequent reaction of these carbon-centred radicals, via O_2-dependent and -independent pathways, to give site-specific strand scission at *N*-acetylglycosamine β-(1 → 4) uronic acid glycosidic bonds (Scheme 1) [10]. The polymer-derived carbon-centred radicals detected by EPR spin trapping in the current study are proposed to be those formed via these processes. The site-specific cleavage mechanisms depicted in Scheme 1 are believed to underlie the formation of the well-defined, low-molecular-mass species detected on polyacrylamide gels.

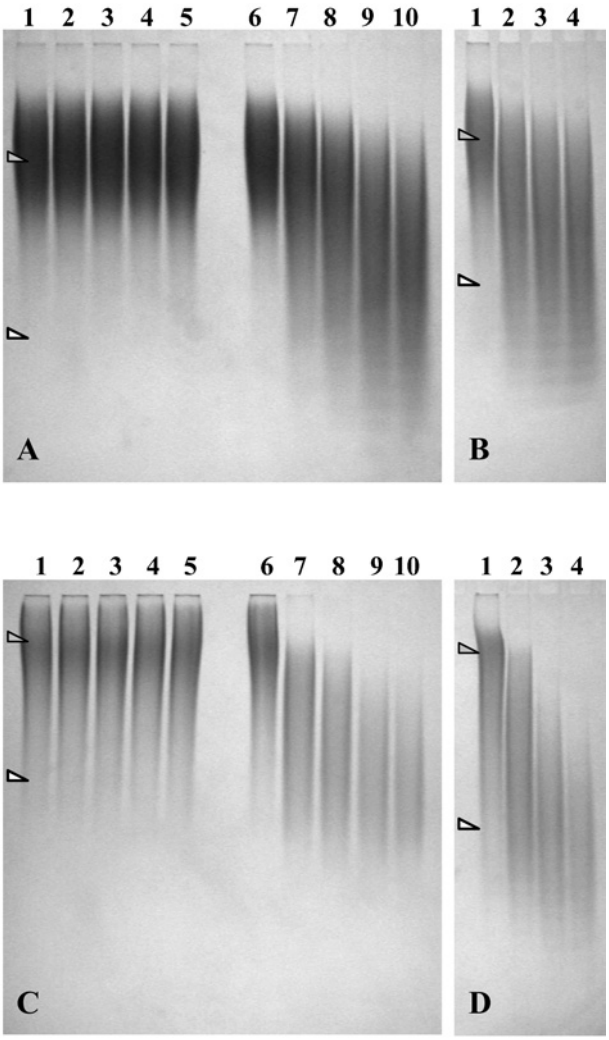

Figure 5 Time- and concentration-dependent depolymerization of glycosaminoglycan chloramides induced by $O_2^{\bullet-}$ at 37 °C and pH 7.4

Polymer samples were analysed using 20 % polyacrylamide gels stained with Alcian Blue as described in the Experimental section. (**A**) Hyaluronan with 1.34 mM SOTS-1 (1.34 mM) after 0, 1, 2, 6 and 24 h incubation (lanes 1–5 respectively) or hyaluronan chloramides (1590 μM) with 1.34 mM SOTS-1 after 0, 1, 2, 6 and 24 h incubation (lanes 6–10 respectively). (**B**) Hyaluronan chloramides (1740 μM) with 0, 0.134, 0.67 or 1.34 mM SOTS-1 (lanes 1–4 respectively). (**C**) As in (**A**) except with chondroitin-4-sulphate and chondroitin-4-sulphate chloramides (730 μM). (**D**) As in (**B**) but with chondroitin-4-sulphate chloramides (740 μM). In all panels, the migration distances of the native glycosaminoglycans (hyaluronan, 120 kDa; chondroitin-4-sulphate, 25–50 kDa) are indicated by grey (upper) darts; the calculated migration distances of the hyaluronan 18-disaccharide (7.2 kDa) and the chondroitin-4-sulphate 12-disaccharide (6 kDa) (see the Experimental section) are indicated by white (lower) darts. Gels shown are representative analyses of three independent experiments.

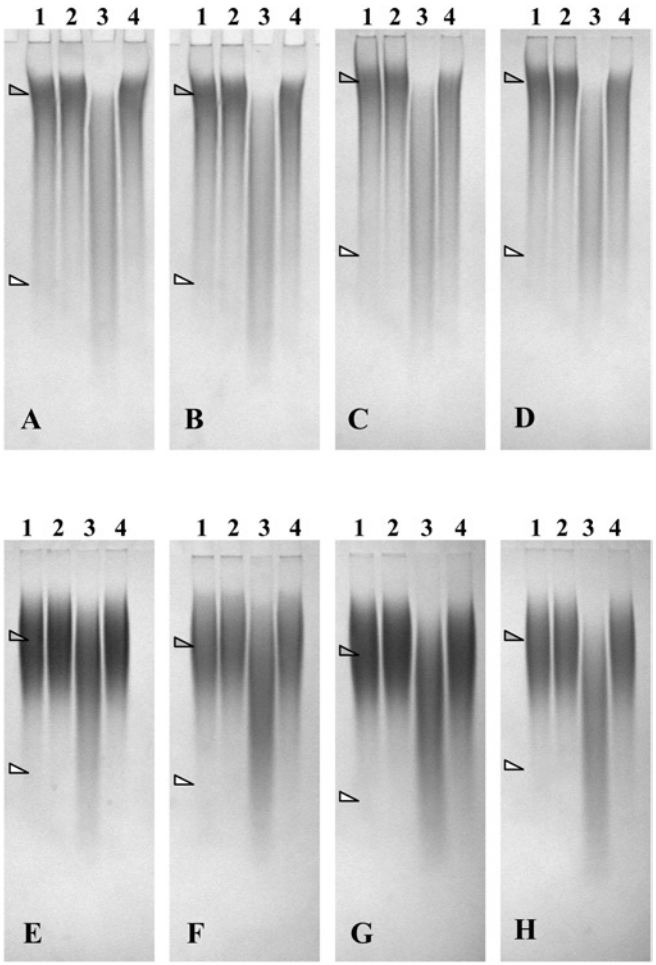

Figure 6 Inhibition of $O_2^{\bullet-}$-dependent depolymerization of glycosaminoglycan chloramides by methionine, SOD, EDTA and BSA at 37 °C and pH 7.4

The concentrations of chloramides in the following incubations were 1590–1740 μM (hyaluronan chloramides) and 600–740 μM (chondroitin-4-sulphate chloramides). (**A**) Hyaluronan chloramides preincubated (22 °C, 15 min) with 0 (lanes 1 and 3) or 8.1 mM methionine (lanes 2 and 4), then with 0 (lanes 1 and 2) or 1.34 mM SOTS-1 (lanes 3 and 4) after 2 h incubation. (**B**) Hyaluronan chloramides with 0 (lanes 1 and 3) or 196 units/ml SOD (0.05 mg/ml) (lanes 2 and 4) and with 0 (lanes 1 and 2) or 1.34 mM SOTS-1 (lanes 3 and 4) after 2 h incubation. (**C**) As in (**B**) except with 500 nM EDTA instead of SOD. (**D**) As in (**B**) except with 0.05 mg/ml BSA instead of SOD. (**E**–**H**) As in (**A**–**D**) but with chondroitin-4-sulphate chloramides. The migration distances are as in Figure 5. Gels shown are representative analyses of three independent experiments.

The protection afforded by SOD (but not inactivated SOD) against chloramide decomposition and polymer fragmentation demonstrates that these processes are $O_2^{\bullet-}$ dependent. This is also consistent with the observed protective effect of DMPO against both chloramide decomposition and polymer fragmentation. SOTS-1-induced polymer fragmentation was shown to be strictly chloramide dependent, as this process did not occur with the native polymers or where the chloramides had been quenched by prior treatment with methionine. Similarly, KO_2 (an authentic source of $O_2^{\bullet-}$) induced fragmentation of hyaluronan chloramides but not the native polymer. In contrast with these $O_2^{\bullet-}$ sources, some chloramide-independent glycosaminoglycan fragmentation was detected with the CH_3CHO–XO system. This fragmentation is consistent with previous results [35], and is attributed to the production of $HO^{\bullet}$ from H_2O_2 (arising from dismutation of $O_2^{\bullet-}$) via a metal ion-catalysed Haber–Weiss reaction [36]. Contaminating metal ions, which may catalyse this reaction, are known to be present in many commercial samples of XO and are extremely difficult to remove [22].

$O_2^{\bullet-}$ may react directly with the glycosaminoglycan chloramides (pathway A, Scheme 2) or via an indirect pathway catalysed by trace (contaminating) transition metal ions (pathway B, Scheme 2). Evidence was provided previously that reaction of other chloramides with $O_2^{\bullet-}$ occurs via both these pathways [12]. Although the buffers used to prepare each of the reagent solutions were treated with Chelex resin to remove transition metal ions, low levels of these species may be present bound to

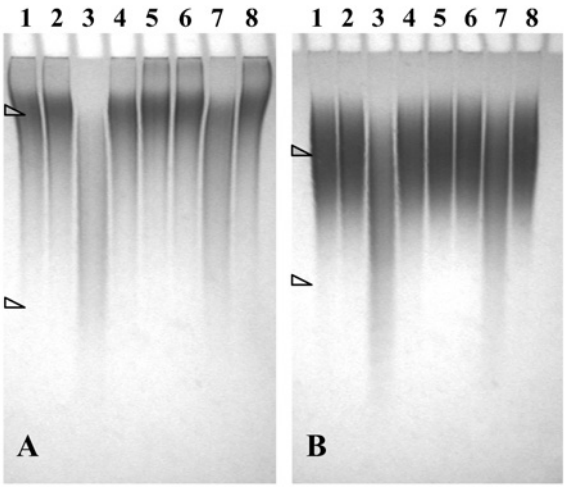

Figure 7 Inhibition of $O_2^{\bullet-}$-dependent depolymerization of glycosaminoglycan chloramides by DMPO at 22 °C and pH 7.4

(**A**) Hyaluronan chloramides (1140 μM) with 0 (lanes 1 and 3) or 102 mM DMPO (lanes 2 and 4) and without (lanes 1 and 2) or with 4.0 mM CH_3CHO and 0.93 unit/ml XO (lanes 3 and 4) after 30 min incubation; lanes 5–8 as in lanes 1–4, except with hyaluronan instead of hyaluronan chloramides. (**B**) Chondroitin-4-sulphate chloramides (480 μM) with 0 (lanes 1 and 3) or 102 mM DMPO (lanes 2 and 4) and without (lanes 1 and 2) or with 4.0 mM CH_3CHO and 0.93 unit/ml XO (lanes 3 and 4) after 30 min incubation; lanes 5–8 as in lanes 1–4 except with chondroitin-4-sulphate instead of chondroitin-4-sulphate chloramides. The migration distances are as in Figure 5. Gels shown are representative analyses of three independent experiments.

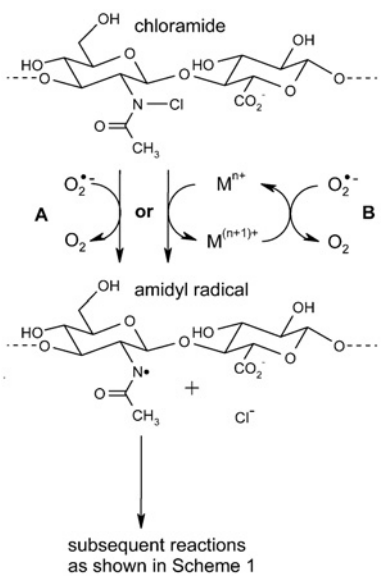

Scheme 2 Proposed mechanism for $O_2^{\bullet-}$-mediated glycosaminoglycan chloramide decomposition (hyaluronan-derived species are shown)

Extensions of the partial structures shown are indicated by dashed bonds. M^{n+} denotes transition metal ion.

the glycosaminoglycans. $O_2^{\bullet-}$ is known to react readily with high-valent transition metal ions such as Cu^{2+} and Fe^{3+} to form Cu^+ and Fe^{2+}. We have previously shown that one-electron reduction of glycosaminoglycan chloramides by low-valent transition metal ions (e.g. Cu^+ and Fe^{2+}) initiates fragmentation of these polysaccharides via the formation of amidyl radicals (cf. Scheme 1) [9,10]. The inhibitory effects of EDTA and BSA on $O_2^{\bullet-}$-induced glycosaminoglycan chloramide decomposition are consistent with this process being metal-ion catalysed. Direct scavenging of $O_2^{\bullet-}$ by EDTA and BSA is unlikely to be responsible for the observed effects since these reactions are slow [37], and low concentrations were employed. It is postulated that EDTA and BSA bind trace metal ions such as Cu^{2+} or Fe^{3+}, initially bound to the polymer chains, in such a fashion as to inhibit either metal-ion reduction by $O_2^{\bullet-}$ or their subsequent reaction with the glycosaminoglycan chloramides. EDTA and BSA have been previously shown to form redox-inactive complexes with Cu^{2+} [38,39], which do not catalyse glycosaminoglycan chloramide decomposition [10]. Fe^{3+}-EDTA is readily reduced by $O_2^{\bullet-}$ [37]; however, it has been shown that the reaction of the (negatively charged) Fe^{2+}-EDTA complex with (negatively charged) glycosaminoglycan chloramides is inefficient [10].

$O_2^{\bullet-}$ is produced in high concentration during the oxidative burst of phagocytes and dismutates to form H_2O_2 [40]; a number of other cells may also generate $O_2^{\bullet-}$ and H_2O_2 at sites of inflammation [41]. $O_2^{\bullet-}$ may also be generated via elimination reactions of alkylperoxyl radicals that are ubiquitous intermediates in the aerobic oxidation of polysaccharides, proteins and DNA [42,43]. Previous studies with model sugar compounds suggest that $O_2^{\bullet-}$ may be eliminated from the glycosaminoglycan-derived peroxyl radicals that are formed via reactions initiated by glycosaminoglycan amidyl radicals under aerobic conditions (Scheme 1) [10]. The carbon-centred radicals generated on rearrangement of glycosaminoglycan amidyl radicals can also undergo β-scission reactions to yield $CO_2^{\bullet-}$ [10], which can rapidly reduce O_2 to $O_2^{\bullet-}$ [44]. It is believed that $O_2^{\bullet-}$ produced in such reactions and/or low-valent transition metal ions generated on metal ion reduction by $O_2^{\bullet-}$ may stimulate further chloramide decomposition. Consistent with the occurrence of such chain reactions, the SOTS-1-induced losses of the glycosaminoglycan chloramides were approximately equal to or greater than the theoretical yields of $O_2^{\bullet-}$ from SOTS-1 under the conditions employed.

The generation of $O_2^{\bullet-}$ by activated phagocytes is accompanied by the release of MPO that converts H_2O_2 into HOCl in the presence of physiological concentrations of Cl^- ions [21]. Since the highly basic (cationic) MPO binds avidly to the negatively charged glycosaminoglycans of the ECM [14–17], it is expected that this material would be an important target for oxidation by MPO-derived HOCl; evidence has been obtained in support of this hypothesis [45]. Transition metal ions such as Cu^{2+} and Fe^{3+} have also been detected at high levels at inflammatory foci [46–48]. These metal ions can form stable complexes with glycosaminoglycans [18,19] and are, therefore, probably available to catalyse $O_2^{\bullet-}$-dependent glycosaminoglycan degradation. Reaction of ECM obtained from cell cultures and healthy pig aortae with HOCl has been shown to result in the fragmentation of matrix proteins and glycosaminoglycans in a manner consistent with the formation and decay of polymer-bound N-chloro species (chloramines/chloramides) [20].

It is known that hyaluronan fragments accumulate at sites of inflammation and tissue injury [49–52], as do modified/fragmented versions of other matrix components including chondroitin sulphates [53–55]. Glycosaminoglycan fragments may be produced via the action of hyaluronidases [56], which can be increased at sites of disease [57]. However, the oxidation of glycosaminoglycans by HOCl and $O_2^{\bullet-}$, via the processes outlined in the present study, is also a potential source of glycosaminoglycan fragments at inflammatory foci, where these oxidants are produced concurrently.

The HOCl-mediated oxidative modification/fragmentation of ECM may have important biological consequences. It is known that changes in (non-modified) matrix components can have profound effects on cell adhesion, proliferation, growth and cell

phenotype [13,58,59], as can oxidation of normal matrix components [60]. Whereas highly polymerized hyaluronan is biologically relatively benign [61], low-molecular-mass hyaluronan oligosaccharides have major biological effects: notably, they appear to play a role in the recruitment and activation of inflammatory macrophages, which may result in an exacerbation of the inflammatory process and tissue damage [49,62–65].

We are grateful to the Australian Research Council and the National Health and Medical Research Council for financial support. M.D.R. gratefully acknowledges an Australian Postgraduate Award administered through the University of Sydney. We thank Professor C. Easton for the gift of SOTS-1.

REFERENCES

1 Libby, P. (2002) Inflammation in atherosclerosis. Nature (London) **420**, 868–874
2 Baker, M. S. (1994) Free radicals and connective tissue damage. In Free Radical Damage and its Control (Rice-Evans, C. A., ed.), pp. 301–317, Elsevier, Amsterdam
3 Waddington, R. J., Moseley, R. and Embery, G. (2000) Reactive oxygen species: a potential role in the pathogenesis of periodontal diseases. Oral Dis. **6**, 138–151
4 Raats, C. J. I., van den Born, J. and Berden, J. H. M. (2000) Glomerular heparan sulfate alterations: mechanisms and relevance for proteinuria. Kidney Int. **57**, 385–400
5 Weiss, S. J., Lampert, M. B. and Test, S. T. (1983) Long-lived oxidants generated by human neutrophils: characterization and bioactivity. Science **222**, 625–627
6 Hawkins, C. L. and Davies, M. J. (1998) Hypochlorite-induced damage to proteins: formation of N-centred radicals from lysine residues and their role in protein fragmentation. Biochem. J. **332**, 617–625
7 Prutz, W. A. (1996) Hypochlorous acid interactions with thiols, nucleotides, DNA, and other biological substrates. Arch. Biochem. Biophys. **332**, 110–120
8 Hawkins, C. L. and Davies, M. J. (2002) Hypochlorite-induced damage to DNA, RNA, and polynucleotides: formation of chloramines and nitrogen-centered radicals. Chem. Res. Toxicol. **15**, 83–92
9 Hawkins, C. L. and Davies, M. J. (1998) Degradation of hyaluronic acid, poly- and monosaccharides, and model compounds by hypochlorite: evidence for radical intermediates and fragmentation. Free Radic. Biol. Med. **24**, 1396–1410
10 Rees, M. D., Hawkins, C. L. and Davies, M. J. (2003) Hypochlorite-mediated fragmentation of glycosaminoglycans and related N-acetyl glycosamines: evidence for chloramide formation, free radical transfer reactions and site-specific fragmentation. J. Am. Chem. Soc. **125**, 13719–13733
11 Fosang, A. J. (1996) Matrix proteoglycans. In Extracellular Matrix: Molecular Components and Interactions, vol. 2 (Comper, W. D., ed.), pp. 200–229, Harwood Academic, Amsterdam
12 Hawkins, C. L., Rees, M. D. and Davies, M. J. (2002) Superoxide radicals can act synergistically with hypochlorite to induce damage to proteins. FEBS Lett. **510**, 41–44
13 Raines, E. W. (2000) The extracellular matrix can regulate vascular cell migration, proliferation, and survival: relationships to vascular disease. Int. J. Exp. Pathol. **81**, 173–182
14 Green, S. P., Baker, M. S. and Lowther, D. A. (1990) Depolymerization of synovial fluid hyaluronic acid (HA) by the complete myeloperoxidase (MPO) system may involve the formation of a HA–MPO ionic complex. J. Rheumatol. **17**, 1670–1675
15 Daphna, E. M., Michaela, S., Eynat, P., Irit, A. and Rimon, S. (1998) Association of myeloperoxidase with heparin: oxidative inactivation of proteins on the surface of endothelial cells by the bound enzyme. Mol. Cell. Biochem. **183**, 55–61
16 McGowan, S. E. (1990) Mechanisms of extracellular matrix proteoglycan degradation by human neutrophils. Am. J. Respir. Cell Mol. Biol. **2**, 271–279
17 Hazell, L. J., Arnold, L., Flowers, D., Waeg, G., Malle, E. and Stocker, R. (1996) Presence of hypochlorite-modified proteins in human atherosclerotic lesions. J. Clin. Invest. **97**, 1535–1544
18 Barbucci, R., Magnani, A., Lamponi, S., Mitola, S., Ziche, M., Morbidelli, L. and Bussolino, F. (2000) Cu(II) and Zn(II) complexes with hyaluronic acid and its sulphated derivative. Effect on the motility of vascular endothelial cells. J. Inorg. Biochem. **81**, 229–237
19 Nagy, L., Yamashita, S., Yamaguchi, T., Sipos, P., Wakita, H. and Nomura, M. (1998) The local structures of Cu(II) and Zn(II) complexes of hyaluronate. J. Inorg. Biochem. **72**, 49–55
20 Woods, A. A. and Davies, M. J. (2003) Fragmentation of extracellular matrix by hypochlorous acid. Biochem. J. **376**, 219–227
21 Kettle, A. J. and Winterbourn, C. C. (1997) Myeloperoxidase: a key regulator of neutrophil oxidant production. Redox Rep. **3**, 3–15
22 Ingold, K. U., Paul, T., Young, M. J. and Doiron, L. (1997) Invention of the first azo compound to serve as a superoxide thermal source under physiological conditions: concept, synthesis, and chemical properties. J. Am. Chem. Soc. **119**, 12364–12365
23 Morris, J. C. (1966) The acid ionization constant of HOCl from 5 °C to 35 °C. J. Phys. Chem. **70**, 3798–3805
24 Konya, K. G., Paul, T., Lin, S., Janusz, L. and Ingold, K. U. (2000) Laser flash photolysis studies on the first superoxide thermal source. First direct measurements of the rates of solvent-assisted 1,2-hydrogen atom shifts and a proposed new mechanism for this unusual rearrangement. J. Am. Chem. Soc. **122**, 7518–7527
25 Prutz, W. A. (1999) Consecutive halogen transfer between various functional groups induced by reaction of hypohalous acids: NADH oxidation by halogenated amide groups. Arch. Biochem. Biophys. **371**, 107–114
26 Hawkins, C. L. and Davies, M. J. (1998) Reaction of HOCl with amino acids and peptides: EPR evidence for rapid rearrangement reactions of nitrogen-centred radicals. J. Chem. Soc. Perkin Trans. 2, 1937–1945
27 Thomas, E. L., Grisham, M. B. and Jefferson, M. M. (1986) Preparation and characterization of chloramines. Methods Enzymol. **132**, 569–585
28 Bernofsky, C., Bandara, B. M. and Hinojosa, O. (1990) Electron spin resonance studies of the reaction of hypochlorite with 5,5-dimethyl-1-pyrroline-*N*-oxide. Free Radic. Biol. Med. **8**, 231–239
29 Min, H. and Cowman, M. K. (1986) Combined Alcian Blue and silver staining of glycosaminoglycans in polyacrylamide gels: application to electrophoretic analysis of molecular weight distribution. Anal. Biochem. **155**, 275–285
30 Cowman, M. K., Slahetka, M. F., Hittner, D. M., Kim, J., Forino, M. and Gadelrab, G. (1984) Polyacrylamide-gel electrophoresis and Alcian Blue staining of sulfated glycosaminoglycan oligosaccharides. Biochem. J. **221**, 707–716
31 Turner, R. E. and Cowman, M. K. (1985) Cationic dye binding by hyaluronate fragments: dependence on hyaluronate chain length. Arch. Biochem. Biophys. **237**, 253–260
32 Finkelstein, E., Rosen, G. M. and Rauckman, E. J. (1980) Spin trapping. Kinetics of the reaction of superoxide and hydroxyl radicals with nitrones. J. Am. Chem. Soc. **102**, 4994–4999
33 Nakao, L. S., Kadiiska, M. B., Mason, R. P., Grijalba, M. T. and Augusto, O. (2000) Metabolism of acetaldehyde to methyl and acetyl radicals: *in vitro* and *in vivo* electron paramagnetic resonance spin-trapping studies. Free Radic. Biol. Med. **29**, 721–729
34 Buettner, G. R. (1987) Spin trapping: ESR parameters of spin adducts. Free Radic. Biol. Med. **3**, 259–303
35 Greenwald, R. A. and Moy, W. W. (1980) Effect of oxygen-derived free-radicals on hyaluronic acid. Arthritis Rheum. **23**, 455–463
36 Haber, F. and Weiss, J. (1934) The catalytic decomposition of hydrogen peroxide by iron salts. Proc. R. Soc. London A **147**, 332–352
37 Bielski, B. H. J., Cabelli, D. E., Arudi, R. L. and Ross, A. B. (1985) Reactivity of HO_2/O_2^- radicals in aqueous solution. J. Phys. Chem. Ref. Data **14**, 1041–1100
38 Cotton, F. A. and Wilkinson, G. (1972) Advanced Inorganic Chemistry, John Wiley and Sons, New York
39 Marx, G. and Chevion, M. (1986) Site-specific modification of albumin by free radicals. Reaction with copper(II) and ascorbate. Biochem. J. **236**, 397–400
40 Henderson, L. M. and Chappell, J. B. (1996) NADPH oxidase of neutrophils. Biochim. Biophys. Acta **1273**, 87–107
41 Medina, M. A., del Castillo-Olivares, A. and Nunez de Castro, I. (1997) Multifunctional plasma membrane redox systems. Bioessays **19**, 977–984
42 von Sonntag, C. (1987) The Chemical Basis of Radiation Biology, Taylor and Francis, London
43 Davies, M. J. and Dean, R. T. (1997) Radical-Mediated Protein Oxidation: from Chemistry to Medicine, Oxford University Press, Oxford
44 Neta, P. and Huie, R. E. (1988) Rate constants for reactions of inorganic radicals in aqueous solution. J. Phys. Chem. Ref. Data **17**, 1027–1284
45 Woods, A., Linton, S. M. and Davies, M. J. (2003) Detection of HOCl-mediated protein oxidation products in the extracellular matrix of human atherosclerotic plaques. Biochem. J. **370**, 729–735
46 Yuan, X. M. and Brunk, U. T. (1998) Iron and LDL-oxidation in atherogenesis. APMIS **106**, 825–842
47 Sayre, L. M., Perry, G., Harris, P. L., Liu, Y., Schubert, K. A. and Smith, M. A. (2000) *In situ* oxidative catalysis by neurofibrillary tangles and senile plaques in Alzheimer's disease: a central role for bound transition metals. J. Neurochem. **74**, 270–279
48 Stadler, N., Lindner, R. A. and Davies, M. J. (2004) Direct detection and quantification of transition metal ions in human atherosclerotic plaques: evidence for the presence of elevated levels of iron and copper. Arterioscler. Thromb. Vasc. Biol. **24**, 949–954
49 McKee, C. M., Penno, M. B., Cowman, M., Burdick, M. D., Strieter, R. M., Bao, C. and Noble, P. W. (1996) Hyaluronan (HA) fragments induce chemokine gene expression in alveolar macrophages. The role of HA size and CD44. J. Clin. Invest. **98**, 2403–2413

50 Balazs, E. A., Watson, D., Duff, I. F. and Roseman, S. (1967) Hyaluronic acid in synovial fluid. I. Molecular parameters of hyaluronic acid in normal and arthritis human fluids. Arthritis Rheum. **10**, 357–376
51 Bjermer, L., Lundgren, R. and Hallgren, R. (1989) Hyaluronan and type III procollagen peptide concentrations in bronchoalveolar lavage fluid in idiopathic pulmonary fibrosis. Thorax **44**, 126–131
52 Horton, M. R., Burdick, M. D., Strieter, R. M., Bao, C. and Noble, P. W. (1998) Regulation of hyaluronan-induced chemokine gene expression by IL-10 and IFN-γ in mouse macrophages. J. Immunol. **160**, 3023–3030
53 Kramsch, D. M. and Hollander, W. (1973) The interaction of serum and arterial lipoproteins with elastin of the arterial intima and its role in the lipid accumulation in atherosclerotic plaques. J. Clin. Invest. **52**, 236–247
54 Kramsch, D. M., Franzblau, C. and Hollander, W. (1974) Components of the protein–lipid complex of arterial elastin: their role in the retention of lipid in atherosclerotic lesions. Adv. Exp. Med. Biol. **43**, 193–210
55 Wagner, W. D., Salisbury, B. G. J. and Rowe, H. A. (1987) A proposed structure of chondroitin 6-sulfate proteoglycan of human normal and adjacent atherosclerotic plaque. Arteriosclerosis **6**, 407–417
56 Lokeshwar, V. B., Iida, N. and Bourguignon, L. Y. (1996) The cell adhesion molecule, GP116, is a new CD44 variant (ex14/v10) involved in hyaluronic acid binding and endothelial cell proliferation. J. Biol. Chem. **271**, 23853–23864
57 Lesley, J., Hascall, V. C., Tammi, M. and Hyman, R. (2000) Hyaluronan binding by cell surface CD44. J. Biol. Chem. **275**, 26967–26975
58 Underwood, P. A. and Bennett, F. A. (1993) The effect of extracellular matrix molecules on the *in vitro* behaviour of bovine endothelial cells. Exp. Cell Res. **205**, 311–319
59 Underwood, P. A., Bean, P. A. and Whitelock, J. M. (1998) Inhibition of endothelial cell adhesion and proliferation by extracellular matrix from vascular smooth muscle cells: role of type V collagen. Atherosclerosis **141**, 141–152
60 Vissers, M. C. M. and Thomas, C. (1997) Hypochlorous acid disrupts the adhesive properties of subendothelial matrix. Free Radic. Biol. Med. **23**, 401–411
61 Laurent, T. C., Laurent, U. B. and Fraser, J. R. (1995) Functions of hyaluronan. Ann. Rheum. Dis. **54**, 429–432
62 Noble, P. W., Lake, F. R., Henson, P. M. and Riches, D. W. (1993) Hyaluronate activation of CD44 induces insulin-like growth factor-1 expression by a tumor necrosis factor-α-dependent mechanism in murine macrophages. J. Clin. Invest. **91**, 2368–2377
63 Horton, M. R., McKee, C. M., Bao, C., Liao, F., Farber, J. M., Hodge-DuFour, J., Pure, E., Oliver, B. L., Wright, T. M. and Noble, P. W. (1998) Hyaluronan fragments synergize with interferon-γ to induce the C-X-C chemokines mig and interferon-inducible protein-10 in mouse macrophages. J. Biol. Chem. **273**, 35088–35094
64 Horton, M. R., Boodoo, S. and Powell, J. D. (2002) NF-κB activation mediates the cross-talk between extracellular matrix and interferon-γ (IFN-γ) leading to enhanced monokine induced by IFN-γ (MIG) expression in macrophages. J. Biol. Chem. **277**, 43757–43762
65 McKee, C. M., Lowenstein, C. J., Horton, M. R., Wu, J., Bao, C., Chin, B. Y., Choi, A. M. K. and Noble, P. W. (1997) Hyaluronan fragments induce nitric-oxide synthase in murine macrophages through a nuclear factor κB-dependent mechanism. J. Biol. Chem. **272**, 8013–8018

Received 27 January 2004/12 March 2004; accepted 13 April 2004
Published as BJ Immediate Publication 13 April 2004, DOI 10.1042/BJ20040148